Urban Climate 38 (2021) 100907

Contents lists available at ScienceDirect

Urban Climate

journal homepage: www.elsevier.com/locate/uclim

A detectable urbanization effect in observed surface air temperature data series in Pyongyang region, Democratic People's Republic of Korea

Kum-Chol Om [a,*], Guoyu Ren [b,c], Hyon-U Kim [a], Sang-Il Jong [a], O. Nam-Chol [a], Hui-Chol Kim [a]

[a] Department of Meteorology, Faculty of Global Environmental Science, Kim Il Sung University, Pyongyang, Democratic People's Republic of Korea
[b] Department of Atmospheric Science, School of Environmental Studies, China University of Geosciences (CUG), Wuhan 430074, China
[c] Laboratory for Climate Studies, National Climate Center, China Meteorological Administration (CMA), Beijing 100081, China

ARTICLE INFO

Keywords:
Surface air temperature
Observational data
Climate warming
Urbanization effect
Pyongyang region

ABSTRACT

A significant urbanization effect in the observed surface air temperature (SAT) data series have been found in developing regions. Here we analyzed the possible impact of urbanization on long-term SAT trends in the Pyongyang region of the Democratic People's Republic of Korea by using data of SAT, wind data and Landsat TM images. Results show that the annual mean urbanization effect in the SAT series was about 0.051 °C/decade for Pyongyang station, 0.031 °C/decade for stations of medium-size cities, and 0.019 °C/decade for stations of small cities and towns, over the period 1969–2019. The annual mean urbanization contributions to the overall warming ranged from 5.3% to 13.1% for different city stations during the study periods, with Pyongyang station witnessing the largest urbanization contribution. Seasonally, the urbanization effect was the largest during wintertime. Urbanization contributions to trend of extreme temperature events are more evident in cold weather indices than warm indices, which reached nearly one-quarter or one-fifth and even 30%. Compared to China's mainland and Japan, the urbanization effect on the regional SAT trend in the Pyongyang region is smaller, but it is detectable.

1. Introduction

Previous studies have analyzed the spatial and temporal characteristics of global and regional temperature changes (Hansen et al., 2006; Jones et al., 2012). Jones et al. (2012) showed that the annual mean SAT (surface air temperature) in the northern and southern hemispheres increased by 1.12 and 0.84 °C, respectively, between 1901 and 2010. Many works have been also published for the regions and countries surrounding the DPRK, and found a remarkable warming over the past decades especially in wintertime (Sun et al., 2006; Dong et al., 2009; Zhao et al., 2009; Hulme et al., 2010; Vincent et al., 2012; Jo et al., 2019).

A major source of uncertainties in the studies of SAT changes is the effect of urbanization around the observational stations. In recent two decades, extensive studies were carried out to evaluate the urbanization effect in the temperature data series in North America (Zhang et al., 2009; Hardin et al., 2018), Europe (Zhou et al., 2013; Chrysanthou et al., 2014; Manuel et al., 2019) and Asia (Ren et al., 2008; Fujibe, 2009; Yang et al., 2011; Ren et al., 2014; William and Gough, 2016; Kealdrup et al., 2019; Luo and Lau, 2018,

* Corresponding author.
E-mail address: kc.om@ryongnamsan.edu.kp (K.-C. Om).

https://doi.org/10.1016/j.uclim.2021.100907
Received 26 April 2021; Received in revised form 18 June 2021; Accepted 29 June 2021
Available online 10 July 2021

2019, 2021).

Several studies have been conducted for China's mainland to estimate the contribution of urbanization to the observed temperature increase and humidity decrease for varied periods and station groups (e.g. Ren et al., 2008; Zhang et al., 2010; Wang and Ge, 2012; Zhou and Ren, 2012, 2014; Yang et al., 2019; Luo and Lau, 2019, 2021). Ren et al. (2008) classified the data of 282 national climate stations according to the size of urban population and specific locations of stations in order to determine the contribution of urbanization to the temperature rise as estimated for North China over the past decades. They found that the urbanization effect was 0.16 °C/decade for the large city stations and 0.07 °C/decade for the small city and town stations, with the regional averaged urbanization effect in the study area being more than 0.11 °C/decade for all the national stations. Zhang et al. (2010) showed that the annual mean urbanization contribution to the warming trend reached at least 27% for the country-averaged annual mean SAT of 1961–2004 based on 614 Chinese national climate stations which had been most frequently applied in studies of climate change. Ren and Zhou (2014) reported a first result to quantify the contribution of urbanization to the estimated extreme temperature events trends over China's mainland, and they found that urbanization effects are significant for most extreme climate indices during 1961–2008.

Luo and Lau (2021) used temporal variation data of land use/land cover maps to classify the weather stations, and employed 16 heat stress indices to estimate the urbanization effect in China for 1971–2014. Their findings showed that the urbanization effect made an important contribution to entire increase in mean heat stress over main urban-group areas, which accounts for 24.1% of total.

Om et al. (2019) reported for the first time the significant warming of the last almost a hundred years in the DPRK; however, no effort has been yet made to examine the urbanization effect on the currently estimated long-term SAT trends in the country. It would be especially interesting to understand the urbanization effect and contribution in the SAT data series of northern Korean Peninsula, where undergoing urbanization process as other regions of East Asia.

This paper is a first attempt to analyze the urbanization effect on observed surface temperature trends for 1961–2019 over the DPRK. The results of the study will help to deepen our understanding of regional climate change and increase our ability to verify regional climate models usually used for projection of future climate in the Korean Peninsula, and East Asia.

2. Data and methods

2.1. *Study area, stations used and data homogenization*

The study area consists of four towns (Pyongyang, Phyongsong, Hwangju and Songnim) and nine counties (the rest), Pyongyang city, as a special municipality contains 5 stations: Pyongyang station in the mid-town area and the rest in the suburbs.

Meanwhile, from the geographical point of view, there extends a plain of an altitude of 100 m and less to the southwest, account for about 50%, the northeast forms a basin comprised of hills and low mountains. All weather stations located on low-lying area of an altitude of 80 m and below. Among them, the horizontal distance between Kangnam and Mangyongdae station is the shortest, about 10-km, that between Phyongsong station is about 60 km from Hwangju, is the longest one. We first analyzed the majority of weather systems have been impacting on the weather and climate of each station over the study area during the study period, and confirmed the similarity that all stations have been under the same weather systems in case of beyond about 93%. It shows a good precondition for estimating urbanization effect.

Daily mean, minimum and maximum SAT data series of 1969–2019 for all stations and of 1961–2019 for some stations (inc. Pyongyang station) were used to evaluate the urbanization effect in the region. In addition, hourly wind data for 1971—2019 were used for determining the prevailing wind frequency in the present study. The observed weather data for all stations were provided by the State Hydro-Meteorological Administration of DPR Korea (SHMA). SHMA has a relative dense station net on nationwide scale, including above 40 WMO-code weather stations. For the surface air temperature observation, the accuracy of all thermometers installed at the focusing stations is ± 0.1 K, and the observational frequency has a strict regularity with 8 times per a day (one time per an hour since 2016).

The daily temperature data have been quality-controlled, and the missing records of a few of daily temperature data have been interpolated, by the SHMA. The data series as reported in this paper include the time period of the most rapidly climate warming for the globe and East Asia (Jones et al., 2012; Om et al., 2019). Besides, the Landsat TM image data series other than observational weather records were used to evaluate the state of land cover for classification of weather stations.

The wind data of the all stations had already been quality-controlled and corrected by the SHMA. The data were tested for possibly remaining errors and inhomogeneities probably caused by unnatural factors (e.g. lack of records, relocation, change in observation regulation and instrumentation). The quality control and homogenization were made referring to those reported by Aguilar et al. (2003), Brandsma and Können (2006) and Boulanger (2010). No record error was found for wind data series during a re-check of the station data. Most of the SAT stations belong to the provincial capitals or the county seats. These governmental offices keep high quality data and have provided the longest records during the study period.

Most of the SAT stations belong to the provincial capitals or the county seats, which keep the best data quality and the longest records during the study period, while the other stations have missing records. For the missing daily records of a station, we conducted the Pearson correlation (bivariate correlation) analysis to select the neighboring stations that had the best relationships with the target station and to obtain the interpolated value during the data overlap period. The missing daily data were then supplemented by adding or subtracting this value. For example, for stations of Ponghwa, Mangyongdae and Junghwa, missing records account for less than 4.2%, 2.9% and 3.6%, respectively. These missing values were thus interpolated with intact records of the surrounding stations, which have high correlation coefficients of beyond 0.95 with the stations with missing records. This approach is similar to the previous studies by Aguilar et al. (2003), and Brandsma and Können (2006). Collectively, the missing records represented less than 1.3% of the total records in this study, and all of them were supplemented.

The thirteen stations had not experienced any relocation during the study period (Table 1), and preliminary examination referring to the methods of Aguilar et al. (2003) and Brandsma and Können (2006) found no significant breakpoints in the SAT data series probably caused by other artificial factors like instrumentation. Therefore, no adjustment for inhomogeneities was conducted for the SAT data. Compared with those in other neighboring countries, the data inhomogeneities related to the station relocations would not be so serious in the study region, which would result in the gradual worsening of observational settings around the grounds of the stations and frequent relocations of stations in cities, as occurred in China's mainland (Om et al., 2019).

2.2. Methods

We used a new method to identify urban and rural stations in estimation of the urbanization effect in this work. The number and density of population in cities where the stations are located were used to identify urban and rural stations in many previous studies (e.g. Li and Huang, 2013; Shastri et al., 2015). However, merely considering population density is not suitable to describe the scale of urbanization around the stations (Ren et al., 2008; Ren and Zhou, 2014). In this article, we did not focus our effort on the population density of the study area, because of there is no pronounced contrasts between those surrounding the weather stations, excluding Pyongyang station. It implies that the grouping of stations merely using the population-related information such as the number of population and density is not suitable to categorize the urban-rural boundaries over the study area.

An approach called Surface Material Ratio Estimation (hereafter SMRE) was put forward to decide the scale of urbanization impact around the observational sites. The basic idea is to consider the areal ratio ($S_{U/N}$) of urban land cover for a 5-km radius circle around the weather station, which reflects integration of built-up areas to nature land cover near the stations. $S_{U/N}$, as a proportion, is expressed by following formula (1):

$$S_{U/N} = S_{Urban} / S_{Nature} \tag{1}$$

where S_{Urban} means the area of built-up cover around a station, while S_{Nature} indicates the area of natural land cover around the same station. The larger the $S_{U/N}$, the stronger the impact of the urban heat island (UHI) effect on observations, according to the underline principle of the UHI formation. $S_{U/N}$ can thus indicate the intensity of urbanization around the stations. Prior to this study, many researchers regarded the land use, the land cover state and the built-up areal fraction (BAF) for assessing urban heat island intensities over the relevant areas (Ren and Zhou, 2014; Jose et al., 2016; Juan and González-Asensio, 2018; Terence et al., 2017; Foissard et al., 2019; Luciana and Denise, 2019; Tysa et al., 2019; Luo and Lau, 2021).

Tysa et al. (2019) used a comprehensive procedure to account for the distribution of land use and land cover over 16 different circular areas with the observational stations as the centers. Chrysanthou et al. (2014) suggested a method to estimate proportion of urban area surrounding station, and to consider the influence of wind on UHI in setting influential area for classification of the stations. This approach takes account for the segment of the circle upwind of station.

As is well-known, the air temperature change in localities is affected by horizontal, vertical advection and non-adiabatic processes, respectively. Among them, the horizontal advection is the largest in order of magnitude. Hence, local SAT is largely dominated by inflowing cold or hot air advection in a thermodynamic view. When the flow passes through an urban area, it will be heated due to the warmer surface and will affect the SAT of the observed sites downstream. We therefore suggested a method to consider the advection impact on air temperature change of the leeward stations. Considering the wind at assessing urban climate had been also suggested in Yang et al. (2019);

We analyzed wind data for 13 stations and set surrounding circular area 5-km far away from every station as the influential area so as not to overlay with neighboring one (Table S1 of Supplementary Information and Fig. 1). In general, the size of footprint area can be varied with the localities and researchers. For example, in previous studies, Ren and Zhou (2014) chose the buffering footprint area of 2-km radius, Luo and Lau (2018) used the time-varying BAF within the 7-km buffer circle around the station, and Mishra et al. (2015)

Table 1
Information of the stations used in the study.

Station name	Code	Longitude (E)	Latitude (N)	Altitude (m[a])	Start
Pyongyang	**47,058**	125° 47′	39° 02′	36.19	1907/01/01
Phyongsong	99,103	125° 53′	39° 15′	80.70	1969/01/01
Mangyongdae	99,100	125° 38′	38° 59′	5.00	1969/01/01
Ponghwa	99,115	125° 59′	39° 09′	23.95	1954/09/01
Samdung	99,116	126° 12′	38° 59′	69.81	1956/01/01
Kangnam	99,164	125° 38′	38° 55′	18.56	1969/01/01
Junghwa	99,128	125° 43′	38° 51′	40.03	1968/06/01
Taedong	99,121	125° 32′	39° 05′	16.83	1969/09/21
Kangso	99,129	125° 31′	38° 56′	24.25	1968/09/01
Sungho	99,163	125° 59′	38° 59′	12.57	1968/06/01
Sangwon	99,127	126° 05′	38° 50′	55.06	1968/08/01
Songnim	99,506	125° 37′	38° 45′	30.06	1967/11/01
Hwangju	99,507	125° 45′	38° 42′	29.67	1968/12/01

[a] Above sea level. Bold indicates WMO station code, and others are domestic codes.

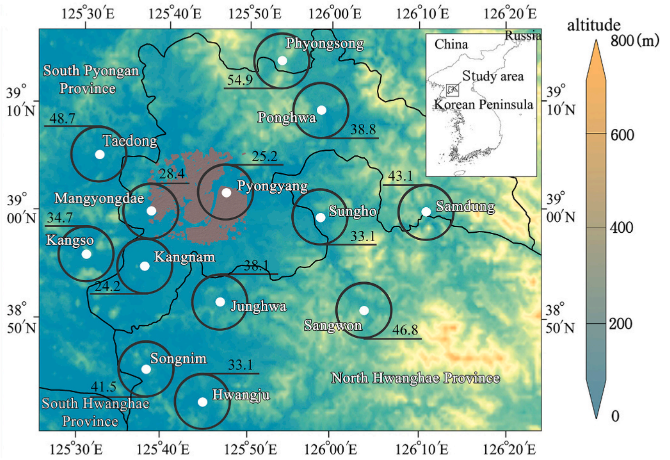

Fig. 1. Study region with the geographical locations of 13 weather stations. Black solid line, boundary of administrative section; light brown block, built-up area; black circular line, influential area; white small circle, weather station; underline value, calm weather frequency (%) for 1971–2019; built-up areas of other cities and towns are abbreviated for brevity in the figure. (For interpretation of the references to colour in this figure legend, the reader is referred to the web version of this article.)

selected the surrounding area of 25-km as the extent of the buffer zone. Meanwhile, Luo and Lau (2019) confirmed that such differences in the selection of BAF could not lead to remarkably differing UHI scales, with testing the sensitivity of the results for several buffering radii of 3, 5, 7 and 9-km.

Fig. 1 shows that the mean calm weather (hourly mean wind speed below 0.5 m/s) frequency for 12 stations is 37% and particular

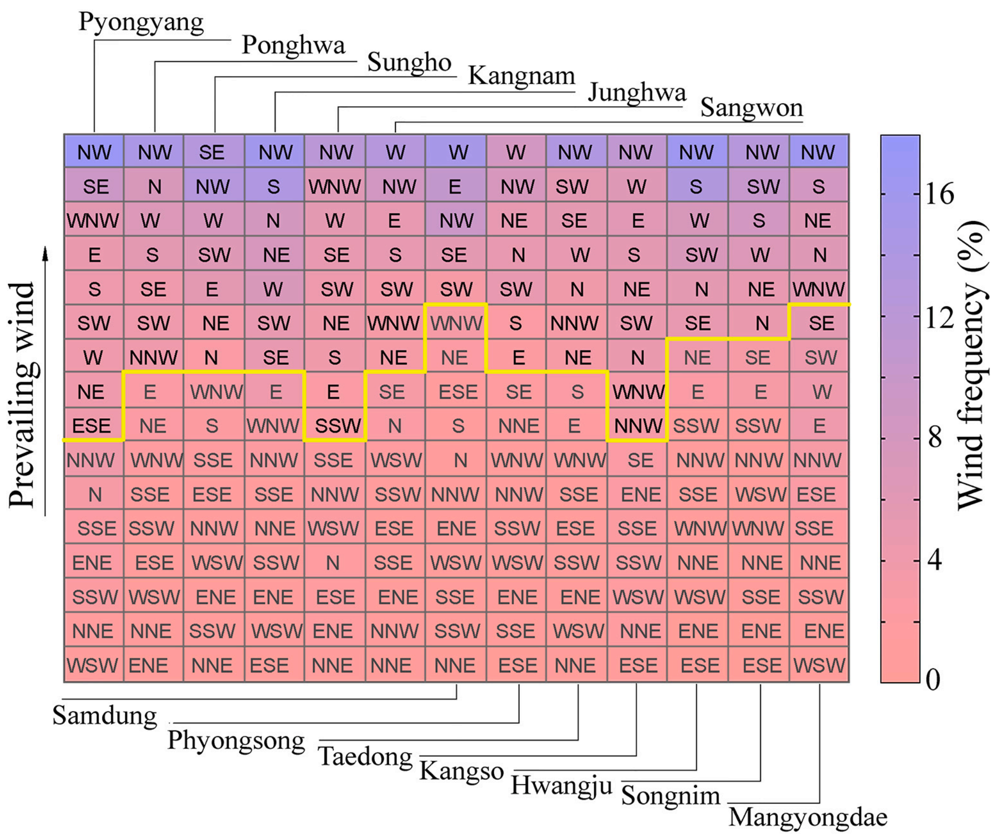

Fig. 2. Prevailing winds and their frequencies for 13 weather stations. Yellow line, boundary of cumulative frequency 70%; top and bottom underline indicates names of the weather stations. (For interpretation of the references to colour in this figure legend, the reader is referred to the web version of this article.)

stations are below 50% excluding Phyongsong station, which implies that the UHI around the stations is somewhat influenced by wind during about two-thirds of days and there is a need to reset each influential area to classify stations. So we analyzed the wind frequency of different directions and obtained rose maps for the 13 stations, and the results are shown in Fig. 2.

We fixed the threshold of cumulative frequency as 70%, because the threshold can reflect relatively the windy characteristic, but the results had no change with increasing threshold. Most of the stations showed that NW and W winds are the first and second prevailing winds, respectively.

We then determined the amendment amount of CPEA (Center Point of Effected Area) toward the upwind for 13 stations (Figs. 3 and 4). This CPEA control method is based on an idea that the relocation of footprint area toward the representative upwind can reflect better influence of the land cover state on SAT over focusing station. Here, we calculated mean frequency for wind directions beyond 70% of cumulative frequency for each station, and then determined relocation distance toward mean upwind on the basis of wind rose map. Moving distance D_{reloc} is decided by following formula (2):

$$D_{reloc} = (fre_{move}/fre_{total})*Rad_5 \tag{2}$$

where fre_{total} is the total cumulative frequency for represent wind (above 70%), fre_{move} is the frequency for mean upwind directions (e.g. NW-17.4% in Pyongyang station) for each station, respectively, and Rad_5 is the affected area with a 5-km radius as mentioned above. Moving direction is also decided by the mean upwind direction.

The relocation control of CPEA was carried out for each of the stations (please refer to Table S5 of Supplementary Information). Because most of the weather stations had experienced prevailing wind with NW or W, all CPEA relocations also had generally been adjusted toward those directions, excluding Songnim station, where the controlled influential area shifted to the southwest. Importantly, the controlled influential areas for all stations did not overlap. The classification of the stations was based on the controlled influential areas around the observational sites.

As above mentioned, the buffering area of 5-km radius was chosen to categorize the stations in the present paper, with following reason: reflect the land cover for the region surrounding the station as much as possible, with not allowing the overlapped buffering area. In general, the overlapped footprint leads to an overlapped built-up area in different urban scales, which might cause unavoidable somewhat overestimation of the urbanization effect in the neighborhood of big city. Of course, buffering areas with 4, 3 and 2-km radii as above mentioned literatures, which can also avoid the overlapping. However, when relocating of CPEA with considering the observed wind frequencies, it was possible that rather small radii make the focusing station excessively lean to the recess of CPEA or exceed the bound of that. For the study region, we therefore considered that the 5-km radius is a marginal and proper distance avoid the exaggerated built-up (natural) area, and it is also close to the larger extents in which the UHI effect can affect the most of the observational stations (Tysa et al., 2019).

We classified the 13 stations into four large groups (big city, medium-size city, small city and rural stations) by using SMRE based on Landsat TM images at 30 × 30 m horizontal resolution. The big city station has a $S_{U/N}$ value $\geqq 1$, medium-size city stations a value 1.0–0.3, small city stations a value 0.3–0.1, and rural stations a value <0.1 (Table 2). According to the analysis of the satellite images, change in land cover over surrounding Pyongyang station since the 1990s are remarkable, especially after 2000s, other cities and towns had experienced somewhat different variations, respectively. We confirmed that the different images result in some differences in land cover and SMRE, but these differences are relatively small, therefore suggested that our category of the weather stations used the land cover is robust. We paid attention to minimize the differences between seasonal effects on the state of land cover, with the Landsat TM data dating on 1992/6/1, 2003/5/31 and 2007/6/3, orbiting on path = 117 and row = 33 and GMT at 01:23:24.06, 02:05:32.17 and 02:11:06.07 used. Using ROI Type Tool of ENVI (v 5.1) software, land cover information of individual images was

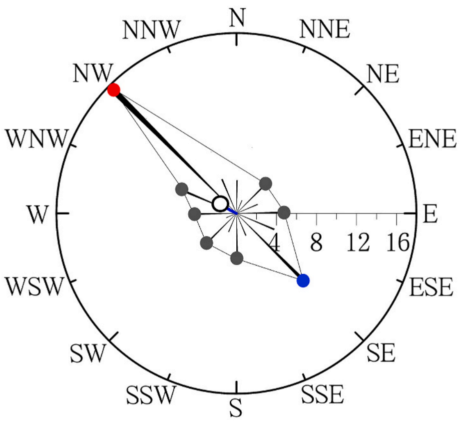

Fig. 3. Analysis of wind rose map at Pyongyang station. Red circle, the first prevailing wind direction; blue circle, the second prevailing wind direction; gray circle, other wind directions; radius axes, wind frequency (%); white circle, amendment for focusing center; blue thick line, controlled moving path of CPEA. (For interpretation of the references to colour in this figure legend, the reader is referred to the web version of this article.)

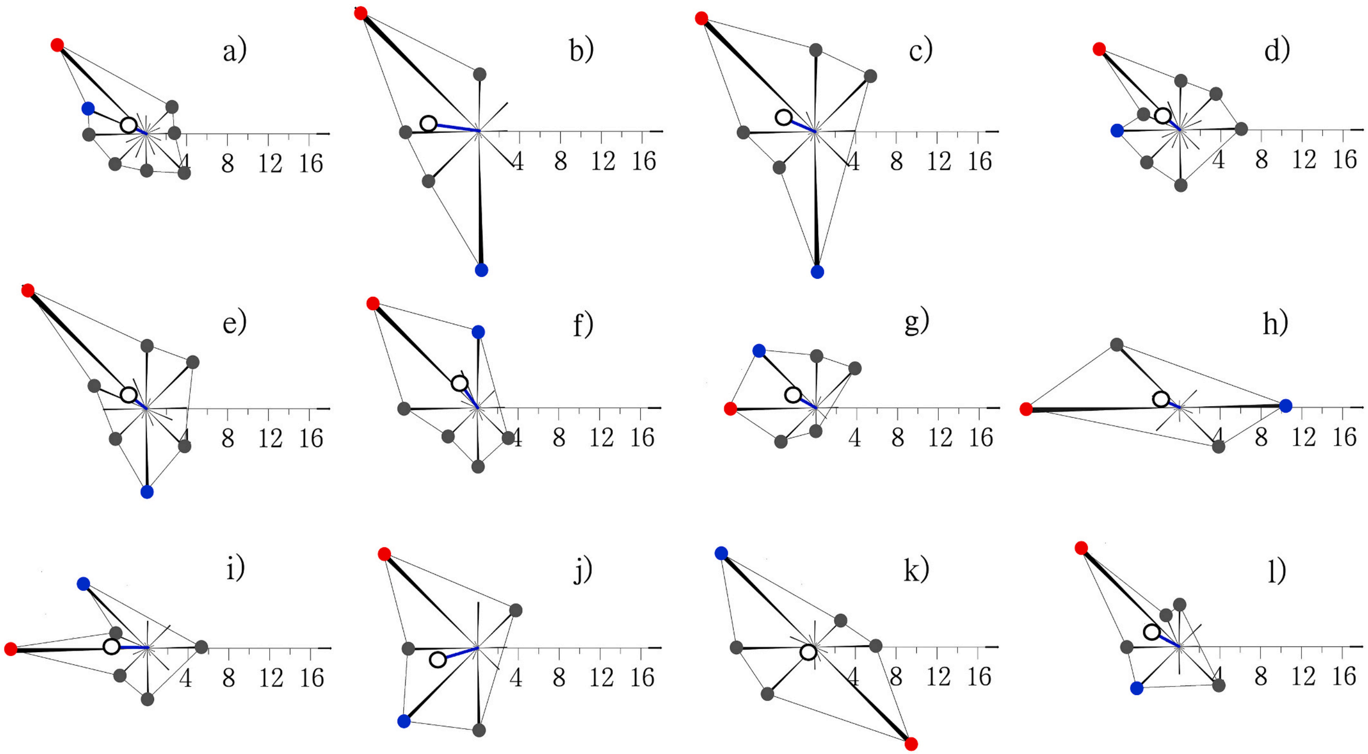

Fig. 4. Wind rose maps and the amendments of CPEA for the stations surrounding Pyongyang. a) ~ l) are Junghwa, Hwangju, Kangnam, Kangso, Mangyongdae, Ponghwa, Phyongsong, Sangwon, Songnim, Sungho and Taedong station, respectively; All symbolic meanings are same as those in Fig. 3. (For interpretation of the references to colour in this figure legend, the reader is referred to the web version of this article.)

Table 2
Classification results of 13 stations in Pyongyang region.

Category	Big city	Medium-size city	Small city/town	Rural
$S_{U/N}$	≧1	1.0–0.3	0.3–0.1	<0.1
Number	1	5	4	3
Station	Pyongyang (1.1)	Mangyongdae (0.6)	Taedong (0.2)	Kangnam (0.07)
		Junghwa (0.7)	Kangso (0.1)	Samdung (0.06)
		Phyongsong (0.7)	Hwangju (0.2)	Ponghwa (0.08)
		Songnim (0.5)	Sungho (0.1)	
		Sangwon (0.3)		

divided into two categories of land cover (natural and built-up areas).

We stipulated that the natural group includes wood, tree and grass, farm fields and water body, and built-up area includes building, pavement, metal and concrete construction, and vehicles. Of course, such classified catalogue is different with other studies, but the result with this approach could explain beyond 92% of land cover information in study area (please refer to Table S6 of Supplementary Information).

Many studies based on remote sensing have been conducted for various areas to identify the differences between urban and rural sites (Zhou et al., 2013; Jose et al., 2016; Yu et al., 2016; Ren and Zhou, 2014). The state of land cover in a given area was used for classification of observational sites in general. Nevertheless, the specific categories of land cover were somewhat different from each other. Overall, the present approach, which takes account of distribution ratio between natural and built-up areas and the actual UHI influential areas of each station by considering prevailing wind directions, has an advantage over those reported previously.

Referring to Ren and Zhou (2014), following formulas (3, 4) were used to calculate the urbanization effect and contribution:

$$\mathrm{UE} = \mathrm{U_T} - \mathrm{U_R} \tag{3}$$

$$\mathrm{UE_s} = (\mathrm{UE}/\mathrm{U_T}) \times 100(\%) \tag{4}$$

where UE is the urbanization effect (°C/decade), U_T is linear trend of annual mean SAT at the urban or town station (°C/decade) and U_R is also that one in the rural station (°C/decade), and UE_s is the contribution of the urbanization effect.

We also calculated the difference series of temperature anomalies between city stations and rural stations (please refer to Table S2, S3 and S4 of Supplementary Information), and estimated the urbanization effect of the city stations by calculating the linear trends of the difference series (Ren and Zhou, 2014; Tysa et al., 2019). The estimates of the urbanization effect by using the above two methods were the same, but the later one permitted us to test the significance of the urbanization effect.

Meanwhile, in order to analyze the possible urbanization effects on the extreme climate events derived from SAT over the study area, we estimated the trends of change in several temperature extreme indices for 1969—2019, all extreme temperature-related indices were selected from ETCCDMI (Expert Team on Climate Change Detection Monitoring and Indices). ETCCDMI offered typical and practical extreme climate indices which were widely used to identify the global and regional extreme weather trends. All extreme temperature-related indices are categorized into three different groups, these are Percentile Based Indices (PBI), Extreme-value Based Indices (EBI) and Threshold Based Indices (TBI), respectively (Table 3). Such similar classifications for indices were reported in other studies (Athar, 2014; Wang et al., 2014). The fourteen indices are calculated based on daily temperature dataset, and their names and definition are shown in Table 3. In Table 3, Annual, TX and TN indicate the period from January 1 to December 31,

Table 3
Extreme temperature indices used in this study.

Indices	Index name	Index definition	Unit
Threshold Based Indices (TBI)			
FD0	Frost days	Annual count of days when TN < 0 °C	Day
ID0	Ice days	Annual count of days when TX < 0 °C	Day
SU25	Summer days	Annual count when TX > 25 °C	Day
TR20	Tropical nights	Annual count of days when TN > 20 °C	Day
Extreme-value Based Indices (EBI)			
TXx	Max TX	Annual maximum value of TX	°C
TNx	Max TN	Annual maximum value of TN	°C
TXn	Min TX	Annual minimum value of TX	°C
TNn	Min TN	Annual minimum value of TN	°C
TXa	Averaged TX	Annual mean value of TX	°C
TNa	Averaged TN	Annual mean value of TN	°C
Percentile Based Indices (PBI)			
TX10	Cold days	Annual count of days when TX < 10th percentile	Day
TX90	Warm days	Annual count of days when TX > 90th percentile	Day
TN10	Cold nights	Annual count of days when TN < 10th percentile	Day
TN90	Warm nights	Annual count of days when TN > 90th percentile	Day

daily maximum temperature and daily minimum temperature, respectively. For calculation of PBI, 1981—2010 was chosen as reference period.

The significance of all the trends was examined by using *t*-test method. The urbanization contribution was calculated only when the urbanization effect was significant statistically.

3. Results

In order to determine the urbanization impact, first we assessed the difference series of SAT between urban and rural stations (Kangnam, Samdung and Ponghwa). The calculation of SAT anomalies in cities of three categories and rural sites was based on the

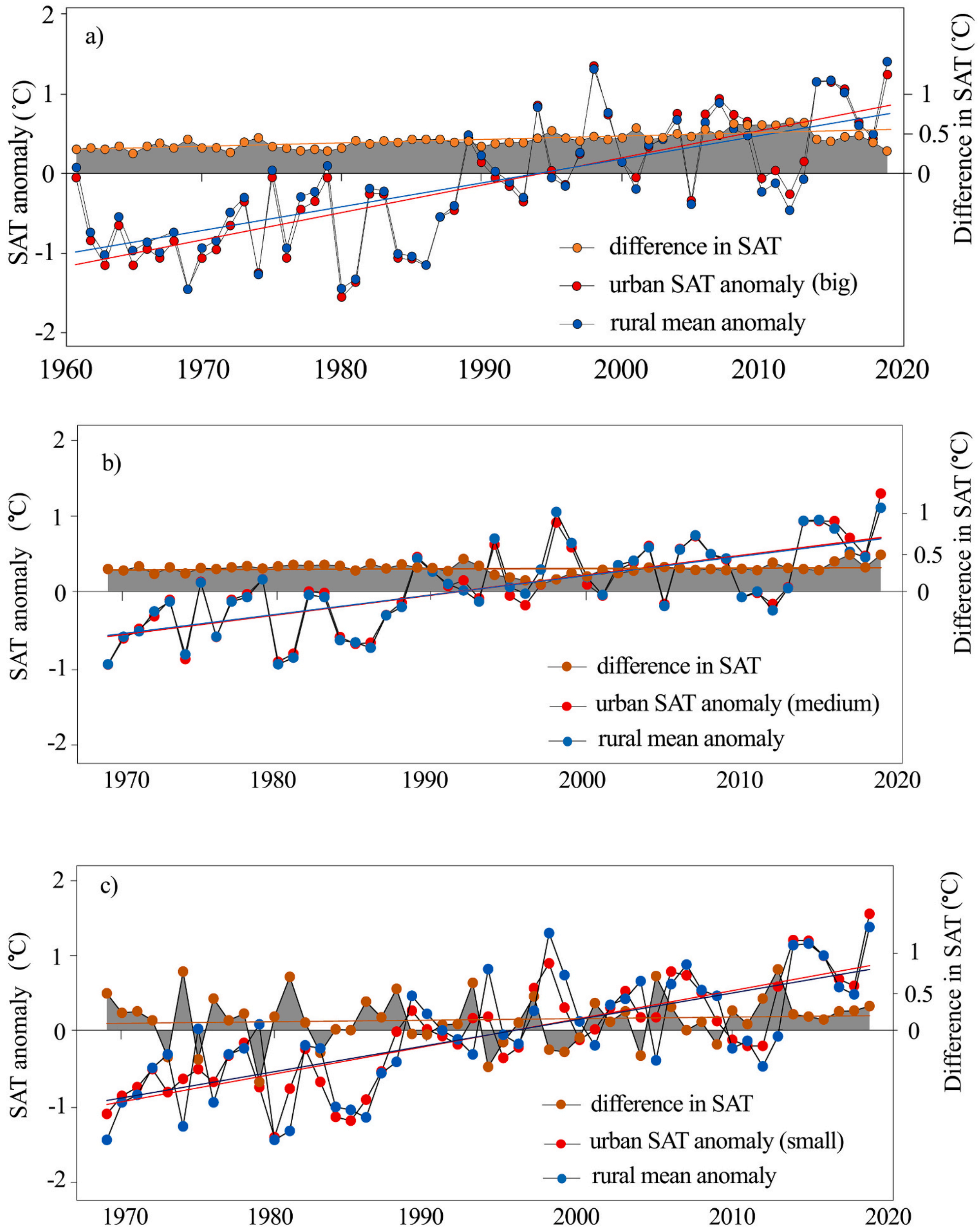

Fig. 5. Difference series of annual mean SAT between the urban stations of three categories the rural stations (Kangnam, Samdung and Ponghwa) and their trends over two periods. Red and blue solid lines denote the linear trends of the urban and rural annual mean SAT anomalies, respectively. a) in case of big city for 1961–2019; b) and c) in case of medium and small city, respectively, for 1969–2019. Gray shading denotes the variation of the urbanization effect, defined as urban minus rural in SAT. (For interpretation of the references to colour in this figure legend, the reader is referred to the web version of this article.)

reference climate period from 1981 to 2010. As shown in Fig. 5(a), the difference series of SAT anomalies between urban and rural stations had a significant rising trend of 0.039 °C/decade for 1961–2019 (orange line), indicating a significant urbanization effect in the urban-station SAT data series (Table 4). Also, medium and small cities had experienced remarkable urbanization effects for 1969–2019 (Fig. 5b and c), with stronger compared to that since 1961 in big city. However, the difference series between urban and rural sites also showed a sudden decrease since 2014, which approximately corresponded to the period of regional warming slowdown in recent years in northeast Asia (Sun et al., 2017). The strengthen winter monsoon circulation and the rising near-surface wind speed (Li et al., 2018; Zhang et al., 2019) may have brought a weakened urbanization effect at the urban stations.

Table 4 shows the estimated results of the SAT trends, urbanization effects and their significances for the different categories and periods of urban and rural sites. Different periods are used due to the difference of observational lengths of the station SAT data.

The urbanization effects in the Pyongyang region were 0.051 °C/decade for big city station or Pyongyang station, 0.031 °C/decade for medium city stations, and 0.019 °C/decade for small city and town stations, during the period 1969–2019. These urbanization effects had different contributions to the overall warming at the city stations. They ranged from 5.3% to 8.4% for different city station groups for the same period, with Pyongyang station witnessing an urbanization contribution of 13.1%. For big city, UE_S is smaller since 1961 than that during 1969—2019, implying that the urban station had experienced a strengthened urbanization effect since the beginning of the 1970s.

Table 5 showed the seasonal mean urbanization contributions for different city stations. UE_S of Pyongyang station were 8.6% in spring, 10.5% in summer, 9.3% in autumn, and 21.3% in winter, respectively, for period 1969–2019. Likewise, the urbanization contributions in winter were the largest for other city groups for both period 1969–2019 and 1961–2019. The least urbanization contributions occurred in summer and spring for Pyongyang station for periods 1961–2019 and 1969–2019. Other city stations also witnessed the least urbanization contribution in summer during 1969–2019. The seasonality of the urbanization effect on SAT trends has been discussed in previous studies, and these results also demonstrate the varied urbanization-related warming for different seasons with the large urbanization effect generally seen in winter in areas of East Asia (e.g. Ren et al., 2007, 2008, Chrysanthou et al., 2014).

While, Table 6 present a more comprehensive analysis for urbanization contribution to the regional climate change over the study area. As shown in Table 6, TBI, EBI and PBI indices, on average, accounted for 25.3%, 19.1% and 20.5% of the variations in relevant temperature indices, respectively, those reached nearly one-quarter or one-fifth of the total trend in big city. Especially, for TNn and TN10p, those showed that big city urbanization contributed to approximately 30% of the entire increasing trend. However, some indices (i.e., TNx, TXn, TNn, TNa and FD0) have not experienced significant differences in change trend between small city and rural sites. For medium-size city, their contributions ranged 5—15% on average. TNn showed the largest trends and contributions in big and medium scale urban sites, which indicates that the urbanization effect largely responds to daily minimum SAT, TNa and TNx also held lead in order of magnitude. Besides, for PBI, the contributions in 10 percentile-related indices were 1.5 times higher than those in 90 percentile ones on the average. From these result, the revaluation of UHI effect basing on daily minimum SAT series rather than daily mean SAT is considerable. Conversely, relative low urbanization effects in warm or hot weather-related indices such as TXx and Warm days (TX90p) may be related with cooling effect due to the irradiance decrease by aerosol emission over the core industrial area during the daytime.

It is still difficult to generalize the urbanization effects found here to that of the entire country because the study area is located in the central part of the DPRK. A weaker urbanization effect may be seen in the northern part of the DPRK where population density is relatively low and many stations are located in mountainous areas. The results, however, are noteworthy in terms of urbanization bias in regional SAT series in the study area.

We also conducted a comparative analysis with those reported in previous works. Zhou and Ren (2009) showed that the urbanization effect was 0.16 °C/decade for the station group of large cities in North China for the period 1961–2000. The urbanization effect at Pyongyang station for the same period was 0.036 °C/decade, which was much smaller than that of large city stations in North China. Recently, Tysa et al. (2019) showed that the urbanization effect for a total of 2286 stations over the whole China accounted for at least 14.6 and 17.1% during 1980–2015 and 1960–2015, respectively and an even larger urbanization contribution had been found for the national reference climate stations and national basic meteorological stations for the same two periods. In the present study, the annual mean contributions were 5.3% for small cities and 13.1% for big city during the period 1969–2019, respectively, which are all smaller than those for the national stations of China's mainland. The difference may be related to the more rapid urbanization processes around the national stations over China's mainland, which may have resulted in a larger increasing rate of urban warming than that over the present study area.

Fujibe (2009) showed that the urban warming in surface air temperature trends as obtained from 561 stations for 27 years (March 1979—February 2006) in Japan was detectable. According to his results, the urbanization contribution for the period was about 10–12%. Although this estimate was almost the same with those obtained in our research, they were actually incomparable because of the different time periods and numbers of stations used between the two analyses. Our analysis and these previous works, however, indicate that the countries and regions outside mainland China might have not been experiencing a rapid urbanization process during the past decades, and the urbanization effects in the currently applied surface air temperature data series were relatively small, though they were still significant.

In order to more accurately detect the changes in SAT in the Korean Peninsula over the last several decades when global warming became more rapid, we would need to pay more attention to the in-depth evaluation of urbanization effect in mean SAT data series in a larger area or the whole Korean Peninsula, and in the main extreme temperature indices series for the country or a larger region. It is also necessary to apply a more sophisticated procedure to classify the stations, considering the possible influence of varied spatial scale urban areas. We would also make an effort to combine the information of population density, built-up area proportion, and mean

Table 4
Surface air temperature trends and urbanization effect for different categories of weather stations.

Period	Indicator	Big city	Medium-size city	Small city/town	Rural
1961—2019	SAT (°C/decade)	0.344**			0.305**
	UE (°C/decade)	0.039*			
	UEs (%)	11.3			
1969—2019	SAT (°C/decade)	0.390**	0.370**	0.358**	0.339**
	UE (°C/decade)	0.051*	0.031*	0.019*	
	UEs (%)	13.1	8.4	5.3	

**: $p < 0.01$; *: $p < 0.05$. UE: Urbanization Effect; UEs: Urbanization contribution.

Table 5
Seasonal mean urbanization contributions (%) for different size city stations.

Period	Season	Big city	Medium-size city	Small city/town
1961—2019	Spring	6.8 (***)		
	Summer	7.5 (***)		
	Autumn	9.3 (***)		
	Winter	22.3 (**)		
1969—2019	Spring	8.6 (***)	7.2 (***)	2.9 (**)
	Summer	10.5 (***)	6.0 (***)	1.3 (***)
	Autumn	9.3 (***)	6.1 (***)	2.7 (***)
	Winter	21.3 (*)	13.2 (**)	13.4 (**)

Asterisk in bracket denotes significance of the urbanization effect, with *** $p < 0.001$, ** $p < 0.01$ and * $p < 0.05$.

Table 6
Trends in extreme climate events and the urbanization contributions (Categories of weather stations and asterisks in bracket are same in Tables 4 and 5, respectively. Trend unit: per decade).

Category	Extreme index	Big city	Medium-size city	Small city/town	Rural
TBI	FD0	−2.6(***)/23.1	−2.4(***)/16.7	−2.0(***)/non	−2.0(***)
	ID0	−2.9(*)/27.6	−2.2(**)/4.5	−2.2(**)/4.5	−2.1(*)
	SU25	4.8(***)/22.9	3.9(***)/5.1	3.6(**)/−2.8	3.7(***)
	TR20	2.9(**)/27.6	2.3(**)/8.7	2.3(**)/8.7	2.1(**)
EBI	TXx	0.30(*)/16.7	0.28(***)/10.7	0.27(**)/7.4	0.25(*)
	TNx	0.28(*)/21.4	0.23(**)/4.3	0.22(*)/non	0.22(*)
	TXn	0.22(**)/4.5	0.22(**)/4.5	0.21(**)/non	0.21(·)
	TNn	0.36(**)/30.6	0.28(**)/10.7	0.25(**)/non	0.25(*)
	TXa	0.24(***)/16.7	0.22(**)/9.1	0.21(*)/4.8	0.20(**)
	TNa	0.32(**)/25.0	0.25(***)/4.0	0.24(*)/non	0.24(*)
PBI	TN10p	−0.80(***)/28.8	−0.63(**)/9.5	−0.54(***)/−5.6	−0.57(**)
	TX10p	−0.46(·)/21.7	−0.39(*)/7.7	−0.39(***)/7.7	−0.36(*)
	TN90p	0.74(**)/17.6	0.62(**)/1.6	0.60(*)/−1.7	0.61(*)
	TX90p	1.07(·)/14.0	0.99(**)/7.1	0.99(*)/7.1	0.92(*)

prevailing wind speed in evaluating and adjusting the urbanization effect of the SAT data by using CPEA method.

4. Conclusions

This paper assessed the urbanization effect on SAT trends in Pyongyang region. The main conclusions were drawn as follows:

(1) To improve estimation of urbanization effect, an approach with considering the direction and frequency of prevailing wind was applied to classify 13 stations over Pyongyang region. All stations were divided into 4 groups (large city, medium city, small city/town and rural stations) based on the new method and satellite images.
(2) Remarkable urbanization effects existed in the SAT data series of urban stations in Pyongyang region during 1961–2019 (1969–2019). For the period 1961–2019, the annual mean urbanization contributions to the overall warming reached 11.3% for Pyongyang station. Since 1969, Pyongyang station had experienced somewhat strengthened urbanization effect, and they were 0.051 °C/decade (13.1%) for stations of big city (Pyongyang), 0.031 °C/decade (8.4%) for stations of medium-size cities, and 0.019 °C/decade (5.3%) for stations of small cities and towns.
(3) By season, the urbanization contributions were 8.6% in spring, 10.5% in summer, 9.3% in autumn, and 21.3% in winter, respectively, since 1969. Winter witnessed the largest urbanization contributions for all the stations and for the two periods analyzed.

(4) Urban area, especially, Pyongyang city experienced more extreme temperature events than the surrounding rural areas, urbanization contribution to increasing trends of representative temperature indices ranged nearly one-quarter or one-fifth, with accounting for nearly 30% of TNn and TN10p as cold(cool) weather-related indices, while some hot (warm) weather-related indices have relatively weaker intensifying uptrends.

It was worth noting that the estimates of urbanization effect and contribution as reported in this paper, as those given in any other studies, were conservative due to the difficulty of identifying real rural stations with observational records long enough for the comparative analysis.

Declaration of Competing Interest

The authors declare that they have no known competing financial interests or personal relationships that could have appeared to influence the work reported in this paper.

Acknowledgments

We are grateful to the State Hydro-Meteorological Administration (SHMA) of DPR Korea for providing the observed daily temperature (mean, maximum and minimum) and hourly wind data of the study area. This work was supported by the National Key Research and Development Program of China (No.2018YFA0605603) and the China University of Geosciences (Wuhan). The calculated data used in this study are available as Supplementary information of the article.

Appendix A. Supplementary data

Supplementary data to this article can be found online at https://doi.org/10.1016/j.uclim.2021.100907.

References

Aguilar, E., Auer, I., Brunet, M., Peterson, T.C., Wieringa, J., 2003. Guidelines on climate metadata and homogenization. In: WCDMP-No. 53, WMO-TD No. 1186, Tech. Rep. World Meteorological Organization.
Athar, H., 2014. Trends in observed extreme climate indices in Saudi Arabia during 1979–2008. Int. J. Climatol. 34, 1561–1574.
Boulanger, J.P., 2010. A procedure for automated quality control and homogenization of historical daily temperature and precipitation data (APACH): part 1: quality control and application to the argentine weather service stations. Clim. Chang. 98 (3), 471–491.
Brandsma, T., Können, G.P., 2006. Application of nearest-neighbor resampling for homogenizing temperature records on a daily to sub-daily level. Int. J. Climatol. 26, 75–89.
Chrysanthou, A., Van der Schrier, G.E.J.M., vanden Besselaar, A.M.G., Tank, Klein, Brandsma, T., 2014. The effects of urbanization on the rise of the European temperature since 1960. Geophys. Res. Lett. 41, 7716–7722. https://doi.org/10.1002/2014GL061154.
Dong, M.Y., Zheng, F.W.U., Jiang, Y., 2009. Comparative analysis of temperature change in the regions of Northeast China and Hokkaido, Japan over the last hundred years. Sci. Geogr. Sin. 29 (5), 684–689.
Foissard, X., Dubreuil, V., Quénol, H., 2019. Defining scales of the land use effect to map the urban heat island in a mid-size European city: Rennes (France). Urban Clim. 29, 100490. https://doi.org/10.1016/j.uclim.2019.100490.
Fujibe, F., 2009. Detection of urban warming in recent temperature trends in Japan. Int. J. Climatol. 29, 1811–1822.
Hansen, J., Sato, M., Ruedy, R., Lo, K., Lea, D.W., Medina-Elizade, M., 2006. Global temperature change. Proc. Natl. Acad. Sci. U. S. A. 103 (39), 14288–14293.
Hardin, A.W., Liu, Y., Cao, G., Vanos, J.K., 2018. Urban heat island intensity and spatial variability by synoptic weather type in the northeast U.S. Urban Clim. 24, 747–762. https://doi.org/10.1016/j.uclim.2017.09.001.
Hulme, M., Zhao, Z., Jiang, T., 2010. Recent and future climate change in East Asia. Int. J. Climatol. 14 (6), 637–658.
Jo, J.S., Pak, S.H., Ri, C.H., Cha, S.O., Kim, G.R., Ri, C.I., Kim, I.S., 2019. Changes in soil properties for 6 years of using the freshwater snail (Ampullaria tischbeini Dohrn) in a reclaimed sodic soil. J. Soils Sediments. https://doi.org/10.1007/s11368-019-02472-7.
Jones, P.D., Lister, D.H., Osborn, T.J., Harpham, C., Salmon, M., Morice, C.P., 2012. Hemispheric and large-scale land surface air temperature variations: an extensive revision and an update to 2010. J. Geophys. Res. 117 (D5), 5127. https://doi.org/10.1029/2011JD017139.
Jose, L., Flores, R., Augusto, J., Pereira, F.H., Karam, A., 2016. Estimation of long term low resolution surface urban heat island intensities for tropical cities using MODIS remote sensing data. Urban Clim. 17, 32–66. https://doi.org/10.1016/j.uclim.2016.04.002.
Juan, A. Acero, González-Asensio, Begoña, 2018. Influence of vegetation on the morning land surface temperature in a tropical humid urban area. Urban Clim. 26, 231–243. https://doi.org/10.1016/j.uclim.2018.09.004.
Li, Q.X., Huang, J.Y., 2013. Effects of urbanization on extreme warmest night temperatures during summer near Bohai. Acta Meteorol. Sin. 27 (6), 808–818.
Li, Y., Chen, Y., Li, Z., Fang, G., 2018. Recent recovery of surface wind speed in Northwest China. Int. J. Climatol. https://doi.org/10.1002/joc.5679.
Luciana, S.F., Denise, H.S.D., 2019. Exploring the relationship between urban form, land surface temperature and vegetation indices in a subtropical megacity. Urban Clim. 27, 105–123. https://doi.org/10.1016/j.uclim.2018.11.002.
Luo, M., Lau, N.C., 2018. Increasing heat stress in urban areas of eastern China: acceleration by urbanization. Geophys. Res. Lett. 45, 13060–13069. https://doi.org/10.1029/2018GL080306.
Luo, M., Lau, N.C., 2019. Urban expansion and drying climate in an urban agglomeration of East China. Geophys. Res. Lett. https://doi.org/10.1029/2019GL082736.
Luo, M., Lau, N.C., 2021. Increasing human-perceived heat stress risks exacerbated by urbanization in China: a comparative study based on multiple metrics. Earth's Future. https://doi.org/10.1029/2020EF001848.
Manuel, D., Jenny, L., Òscar, S., Jan, Esper, 2019. Detection and elimination of UHI effects in long temperature records from villages–a case study from Tivissa, Spain. Urban Clim. 27, 372–383. https://doi.org/10.1016/j.uclim.2018.12.012.
Mishra, V., Ganguly, A.R., Nijssen, B., Lettenmaier, D.P., 2015. Changes in observed climate extremes in global urban areas. Environ. Res. Lett. 10 (2), 024005 https://doi.org/10.1088/1748-9326/10/2/024005.
Om, K.C., Ren, G.Y., Jong, S.I., Li, S.L.O.K.C., Ryang, C.H., Zhang, P.F., 2019. Long-term change in surface air temperature over DPR Korea, 1918–2015. Theor. Appl. Climatol. 138, 363–372.

Ren, G.Y., Zhou, Y.Q., 2014. Urbanization effect on trends of extreme temperature indices of national stations over mainland China, 1961–2008. J. Clim. 27, 2340–2360.

Ren, G.Y., Chu, Z.Y., Chen, Z.H., Ren, Y.Y., 2007. Implications of temporal change in urban heat island intensity observed at Beijing and Wuhan stations. Geophys. Res. Lett. 34, L05711 https://doi.org/10.1029/2006GL027927.

Ren, G.Y., Zhou, Y.Q., Chu, Z.Y., Zhang, A.Y., Guo, J., Liu, X.F., 2008. Urbanization effects on observed surface air temperature trends in North China. J. Clim. 21, 1333–1348.

Shastri, H., Paul, S., Ghosh, S., Karmakar, S., 2015. Impacts of urbanization on Indian summer monsoon rainfall extremes. J. Geophys. Res. Atmos. 120, 495–516. https://doi.org/10.1002/2014JD0220 61.

Sun, F.H., Yang, X.Q., Lu, S., Yang, S.Y., 2006. The contrast analysis on the average and extreme temperature trend in Northeast China. Sci. Meteorol. Sin. 26 (2), 157–163.

Sun, X.B., Ren, G.Y., Ren, Y.Y., Liu, Y.L., Xue, X.Y., 2017. A remarkable climate warming hiatus over Northeast China since 1998. Theor. Appl. Climatol. https://doi.org/10.1007/s00704-017-2205-7.

Terence, D.M., Onisimo, M., John, O., Timothy, D., 2017. Linking major shifts in land surface temperatures to long term land use and land cover changes: a case of Harare, Zimbabwe. Urban Clim. 20, 120–134. https://doi.org/10.1016/j.u clim.2017.04.005.

Tysa, Kealdrup S., Ren, G., Qin, Y., Zhang, P., Ren, Y., Jia, W., Wen, K., 2019. Urbanization effect in regard temperature series based on a remote sensing classification scheme of station. JGR-Atmos. 124 (20), 10646–10661.

Vincent, L.A., Wang, X.L., Milewska, E.J., et al., 2012. A second generation of homogenized Canadian monthly surface air temperature for climate trend analysis. J. Geophys. Res.-Atmos. 117 (D18), 119–130.

Wang, F., Ge, Q.S., 2012. Estimating urban Heat Island effect in China from 1980 to 2009 based on satellite land use changes. Chin. Sci. Bull. 57, 1708–1715. https://doi.org/10.1007/s11434-012-4999-0.

Wang, Q., Zhang, M.J., Wang, S.J., Ma, Q., Sun, M.P., 2014. Changes in temperature extremes in the Yangtze River basin, 1962–2011. J. Geogr. Sci. 24, 59–75. https://doi.org/10.1007/s11442-014-1073-7.

William, A., Gough, Y.H., 2016. Day-to-day temperature variability for four urban areas in China. Urban Clim. 17, 80–88. https://doi.org/10.1016/j.uclim.2016.06.002.

Yang, J., Wang, Y.C., Xiao, X.M., Jin, C., Cecilia, Xia J.H., Li, X.M., 2019. Spatial differentiation of urban wind and thermal environment in different grid sizes. Urban Clim. 28, 100458. https://doi.org/10.1016/j.uclim.2019.100458.

Yang, X., Hou, Y., Chen, B., 2011. Observed surface warming induced by urbanization in East China. J. Geophys. Res. 116, D14113 https://doi.org/10.1029/2010JD015452.

Yu, M., Miao, S., Li, Q., 2016. Synoptic analysis and urban signatures of a heavy rainfall on 7 august 2015 in Beijing. J. Geophys. Res. Atmos. 121 https://doi.org/10.1002/2016JD025420.

Zhang, A.Y., Ren, G.Y., Zhou, J.X., Chu, Z.Y., Ren, Y.Y., Tang, G.L., 2010. Urbanization effect on surface air temperature trends over China. Acta Meteorol. Sin. 68, 957–966 (In Chinese).

Zhang, D.L., Shou, Y.X., Dickerson, R.R., 2009. Upstream urbanization exacerbates urban heat island effects. Geophys. Res. Lett. 36, L24401 https://doi.org/10.1029/2009GL041082.

Zhang, R., Zhang, S., Luo, J., et al., 2019. Analysis of near-surface wind speed change in China during 1958–2015. Theor. Appl. Climatol. 137, 2785–2801. https://doi.org/10.1007/s00704-019-02769-0.

Zhao, C.Y., Ren, G.Y., Zhang, Y.F., et al., 2009. Climate change in Northeast China over the past 50 years. J. Arid Land Res. Environ. 23 (7), 25–30.

Zhou, B., Rybski, D., Kropp, J.P., 2013. On the statistics of urban heat island intensity. Geophys. Res. Lett. 40, 5486–5491. https://doi.org/10.1002/2013GL057320.

Zhou, Y.Q., Ren, G.Y., 2012. Change in extreme temperature events frequency over mainland China during 1961–2008. Clim. Res. 50 (1–2), 125–139.

Zhou, Y.Q., Ren, G.Y., 2014. Urbanization effect on long-term trends of extreme temperature events in North China. Plateau Meteorol. 33 (6), 1589–1958. https://doi.org/10.7552/j.issn.1000-0534. 2013.00153.